Biophysical Journal Volume 86 February 2004 1061–1073

FTIR Difference Spectroscopy in Combination with Isotope Labeling for Identification of the Carbonyl Modes of P700 and $P700^+$ in Photosystem I

Ruili Wang,* Velautham Sivakumar,* T. Wade Johnson,† and Gary Hastings*

*Department of Physics and Astronomy, Georgia State University, Atlanta, Georgia 30303; and †Department of Biochemistry and Molecular Biology, The Pennsylvania State University, University Park, Pennsylvania 16802

ABSTRACT Room temperature, light induced ($P700^+$-P700) Fourier transform infrared (FTIR) difference spectra have been obtained using photosystem I (PS I) particles from *Synechocystis* sp. PCC *6803* that are unlabeled, uniformly ^2H labeled, and uniformly ^{15}N labeled. Spectra were also obtained for PS I particles that had been extensively washed and incubated in D_2O. Previously, we have found that extensive washing and incubation of PS I samples in D_2O does not alter the ($P700^+$-P700) FTIR difference spectrum, even with ~50% proton exchange. This indicates that the P700 binding site is inaccessible to solvent water. Upon uniform ^2H labeling of PS I, however, the ($P700^+$-P700) FTIR difference spectra are considerably altered. From spectra obtained using PS I particles grown in D_2O and H_2O, a (^1H-^2H) isotope edited double difference spectrum was constructed, and it is shown that all difference bands associated with ester/keto carbonyl modes of the chlorophylls of P700 and $P700^+$ downshift 4–5/1–3 cm^{-1} upon ^2H labeling, respectively. It is also shown that the ester and keto carbonyl modes of the chlorophylls of P700 need not be heterogeneously distributed in frequency. Finally, we find no evidence for the presence of a cysteine mode in our difference spectra. The spectrum obtained using ^2H labeled PS I particles indicates that a negative difference band at 1698 cm^{-1} is associated with at least two species. The observed ^{15}N and ^2H induced band shifts strongly support the idea that the two species are the 13^1 keto carbonyl modes of both chlorophylls of P700. We also show that a negative difference band at ~1639 cm^{-1} is somewhat modified in intensity, but unaltered in frequency, upon ^2H labeling. This indicates that this band is not associated with a strongly hydrogen bonded keto carbonyl mode of one of the chlorophylls of P700.

INTRODUCTION

Photosystem I (PS I) catalyzes the light induced transfer of electrons across the thylakoid membrane from plastocyanin to ferredoxin (Golbeck and Bryant, 1991). After light excitation of P700 (the primary electron donor in PS I), an electron is transferred across the membrane via a series of acceptors called A_0, A_1, F_X, F_A, and F_B (Brettel, 1997; Golbeck and Bryant, 1991). In PS I two symmetrical sets of electron transfer (ET) acceptors are bound to the 83 kDa, membrane-spanning subunits, *Psa*A and *Psa*B (Brettel, 1997; Golbeck and Bryant, 1991). It is unclear if ET occurs down one or both branches (Guergova-Kuras et al., 2001; Joliot and Joliot, 1999). It is likely that the directionality of ET in PS I is related to the electronic and structural organization of P700. Light induced Fourier transform infrared (FTIR) difference spectroscopy (DS) is well suited for the direct study of the molecular details of P700 (Breton, 2001; Breton et al., 1999, 2002; Hastings et al., 2001; Kim and Barry, 2000; Kim et al., 2001; Sivakumar et al., 2003), and here we have used FTIR DS in combination with isotope labeling to gain a more detailed understanding of P700.

From the recent crystal structure of PS I at 2.5-Å resolution, P700 is clearly resolved and consists of a chlorophyll-*a* (Chl-*a*) molecule bound to *Psa*B, and a Chl-*a*′ molecule bound to *Psa*A (Fromme et al., 2001; Jordan et al., 2001). The structure and numbering scheme for Chl-*a* is outlined in Fig. 1. Chl-*a*′ is a 13^2 isomer of Chl-*a*. Throughout this article, the two Chls of P700 are termed P_B and P_A. From the 2.5-Å PS I crystal structure it is found that P_A and P_B are asymmetrically bound, with P_A being involved in a hydrogen (H) bond network with several surrounding amino acid residues and a water molecule (Fig. 2; Fromme et al., 2001; Jordan et al., 2001). P_B is not involved in H-bonding.

Fig. 2 shows a view of ring V of P_A taken from the 2.5-Å PS I crystal structure (Fromme et al., 2001; Jordan et al., 2001). Also shown are the nearby amino acid Thr-A743 (Thr-A739 in *Chlamydomonas reinhardtii*) and Tyr-A603. The hydroxyl oxygen of Thr-A743 is 2.98 Å from the 13^1 keto carbonyl (C=O) oxygen of P_A. In addition, the Thr-A743 hydroxyl oxygen is 2.7 Å from the oxygen atom of a water molecule. The angle of 135.8° ($\theta_5 + \theta_6$) between the vectors joining the oxygens (Fig. 2) suggests sp^2 hybridization of the hydroxyl oxygen of Thr-A743. Thus the molecular geometry and the interatomic distances appear to be well suited for the Thr-A743 to form an H-bond to the 13^1 keto C=O oxygen. However, it is unclear how strong this H-bond will be. The strength of the H-bond will depend on the orientation of the water molecule at position 19. In addition, the hydroxyl side chain of Thr-A743 is suitably oriented for the formation of an H-bond to the 13^3 ester oxygen. Given the complexity of the H-bond network shown in Fig. 2, it is possible that the H-bonding of Thr-A743 could be different in the ground and cation states of P700 (see below).

Submitted July 25, 2003, and accepted for publication October 16, 2003.

Address reprint requests to Gary Hastings, Tel.: 404-651-0748; Fax: 404-651-1427; E-mail: ghastings@gsu.edu.

T. Wade Johnson's present address is Susquehanna University, 514 University Ave., Selinsgrove, PA 17870.

0006-3495/04/02/1061/13 $2.00

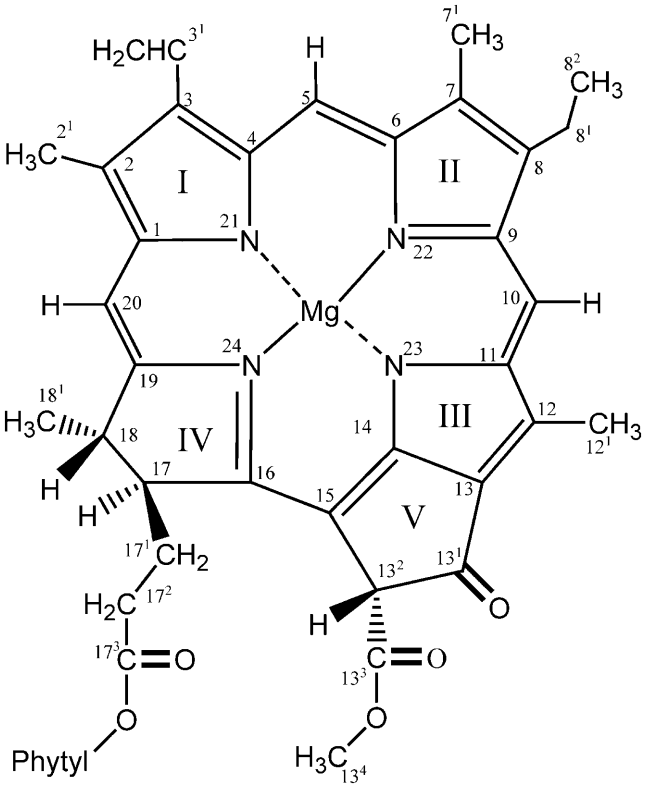

FIGURE 1 Molecular structure and International Union of Pure and Applied Chemistry numbering scheme for chlorophyll-*a*.

Recently, different groups have obtained ($P700^+$-P700) FTIR DS using PS I particles from *Synechocystis* (*S.*) sp. *6803* (Breton, 2001; Breton et al., 1999, 2002; Hastings et al., 2001; Kim and Barry, 2000; Kim et al., 2001) and *C. reinhardtii* (Breton, 2001; Hastings et al., 2001; Redding et al., 1998; Wang et al., 2003; Witt et al., 2002). From these studies different interpretations of the FTIR DS were proposed: 1), On the basis of the observation of multiple band shifts upon specific 13^4 methyl deuteration of ~68% of the Chls in PS I, it was suggested that the 13^3 ester (Kim and Barry, 2000) and 13^1 keto (Kim et al., 2001) carbonyl (C=O) modes of the Chls of P700 are heterogeneously distributed in frequency (the mode frequency is different in different PS I subpopulations). 2), At 90 K, in PS I from *S. 6803*, Breton et al. (1999) suggested band assignments for the 13^1 keto C=O modes of both Chls of P700, that did not involve mode frequency heterogeneity. 3), Recently, we suggested a different set of band assignments for the 13^1 keto C=O modes of the Chls of P700 (Hastings et al., 2001), again without the need to invoke mode frequency heterogeneity. To address these issues we have obtained ($P700^+$-P700) FTIR DS in the 1770–1600 cm^{-1} region using unlabeled (^1H), ^{15}N, and ^2H isotopically labeled PS I particles from *S. 6803*.

Several studies have recently been undertaken to try to establish which difference bands in ($P700^+$-P700) FTIR DS are associated with the 13^1 keto C=O modes of the two Chls of P700. It is important to assign these difference bands unambiguously because they provide a means to estimate the degree of charge delocalization over the chlorophylls of P700.

In (^{3}P700-P700) FTIR DS, obtained using urea treated PS I particles depleted of F_A and F_B at 90 K, Breton et al. (1999) observed a negative difference band at 1637 cm^{-1}. In ($P700^+$-P700) FTIR DS, obtained using intact PS I particles at 90 K, a negative difference band at 1637 cm^{-1} was also observed. These observations led to the conclusion that the 1637 cm^{-1} difference band is due to a 13^1 keto C=O mode of either P_A or P_B. It should be noted that a (^{3}P700-P700) FTIR DS has never been obtained using intact PS I particles,

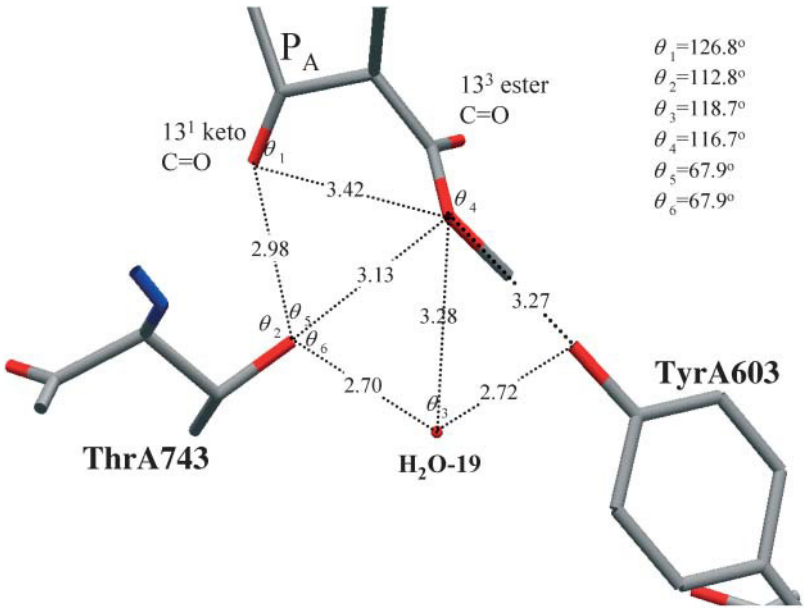

FIGURE 2 View of ring V of P_A showing possible interactions of the 13^1 keto C=O with Thr-A743 (Thr-A739 in *C. reinhardtii*) and water. The H_2O-19 oxygen (*circle*) and Tyr-A603 are also shown. Figure was generated using Swiss PDBViewer and the crystallographic coordinates of PS I at 2.5-Å resolution (PDB file accession number IJB0).

and it was never shown that the triplet state actually studied was associated with one of the Chls of P700.

Given such a low frequency (1637 cm^{-1}) for a 13^1 keto C=O mode, it was proposed that this mode is strongly hydrogen bonded. From the recent PS I crystal structure at 2.5-Å resolution, it has been suggested that the 13^1 C=O mode of P_A could be H-bonded to Thr-A743 (Fig. 2) (Fromme et al., 2001; Jordan et al., 2001). However, it is unclear if the 13^1 C=O mode of P_A is very strongly H-bonded. It is therefore unclear if this interpretation of ($P700^+$-P700) FTIR DS is in agreement with the 2.5-Å PS I crystal structure. Notice also that the above interpretation implies that the triplet state of P700 resides on P_A. This conclusion is inconsistent with recent results on a variety of site directed mutants that clearly indicate that the triplet state of P700 is localized on P_B (Krabben et al., 2000; Webber and Lubitz, 2001).

Given the above interpretation, that the 1637 cm^{-1} band is due to a strongly H-bonded 13^1 keto C=O mode P_A, the charge delocalization over the chlorophylls of P700 was estimated to be ~1.5–2:1 (Breton et al., 1999), which is in stark contrast to the almost completely localized charge distribution that was calculated from ENDOR spectroscopic studies of P700 (Kass et al., 2001, 1998; Webber and Lubitz, 2001).

Within the context of the above interpretation, that the 1637 cm^{-1} band is due to a strongly H-bonded 13^1 keto C=O mode P_A, it is further concluded that a difference band at 1698(−)/1718(+) cm^{-1} is due solely to the free 13^1 keto C=O mode P_B. However, we have found that the 1698 cm^{-1} band splits when the P_A axial histidine ligand (His-A676 in *C. reinhardtii*) is mutated to serine (Hastings et al., 2001). That is, a band that is proposed to be due to 13^1 keto C=O mode $\mathbf{P_B}$ is greatly altered when a mutation is performed near $\mathbf{P_A}$. To explain the splitting of the 1698 cm^{-1} band observed upon mutation of the P_A axial histidine ligand, we suggested that both 13^1 keto C=O modes of the Chls of P700 contribute to the negative difference band near 1698 cm^{-1}, and shift in different directions upon cation formation (Hastings et al., 2001). The oppositely directed shifts possibly being related to changes in H-bond strength of the 13^1 keto C=O group of P_A upon cation formation. With this later interpretation it was also possible to explain the presence of a positive difference band near 1686 cm^{-1} that had hitherto been ignored.

Importantly, if the 1637 cm^{-1} difference band is due to a strongly H-bonded 13^1 keto C=O mode of P_A then this difference band should downshift in spectra obtained using uniformly ^2H labeled PS I particles. Below we will show that this is not observed.

Recently, Witt et al. (2002) have suggested that a difference band at ~1634(−) cm^{-1} upshifted to ~1672 cm^{-1} upon mutation of Thr-A739 (Thr-A743 in *S. 6803*) to valine, tyrosine, or histidine in PS I particles from *C. reinhardtii* (strain CC2696). This observation was interpreted to indicate that the H-bond to the 13^1 keto C=O mode of P_A is removed in all the different Thr-A739 mutants. Several further observations complicate this interpretation, however. First, a frequency of ~1672 cm^{-1} is very low for a presumably free keto C=O mode. Second, no evidence was provided to rule out the possibility that the observed mutation induced changes in the FTIR DS were not a result of reorientation of the peptide backbone. Given the bonding geometry of Thr-A739, removal of this amino acid could impart significant steric freedom to P_A, as well as the immediate protein environment (see Fig. 2). Very recently, we have provided further evidence that suggests that the interpretation proposed by Witt et al. cannot be correct (Wang et al., 2003).

Given the current ambiguities in the precise nature of ($P700^+$-P700) FTIR DS, and in particular, concerning both the frequency and multiplicity of the ester and keto C=O modes of P700, we are embarking on a strategy that involves obtaining FTIR DS using isotopically labeled PS I particles and site directed mutants. As a first step in this approach, here we describe ($P700^+$-P700) FTIR DS obtained using PS I particles from *S. 6803* were obtained from cells grown in D_2O or uniformly ^{15}N labeled media. We also present spectra for PS I particles that have been extensively washed and incubated in D_2O.

MATERIALS AND METHODS

Detergent-isolated PS I particles from *S. 6803* were prepared as described previously (Hastings et al., 1995a, 2001, 1995b). For all FTIR experiments, PS I particles were pelleted and placed between a pair of CaF_2 windows. No mediators were added to the pellet. All experiments described here were performed at room temperature (RT). FTIR spectra were recorded using a Bruker IFS/66 FTIR spectrometer. Sixty-four spectra were collected before and during light excitation from a helium-neon laser. Several spectra were also collected after illumination. The spectra collected before illumination were ratioed directly against the spectra collected during or after illumination. Thus, the absorption spectra collected represent true difference spectra. The dark-light-dark cycle was repeated 200–400 times and all spectra were averaged.

For D_2O exchange experiments, PS I samples in H_2O buffer were pelleted and resuspended in otherwise identical D_2O buffer. These samples were then pelleted using ultracentrifugation and resuspended again in ~10 vol D_2O buffer. The mixture was then refrigerated at 4°C for between 1 h and up to 30 days in the dark. The extent of ^2H exchange was monitored via the intensity of the amide II absorption band (see below). The amide II absorption band was virtually unchanged after the first day of incubation, and the PS I particles were still fully active after 30 days of incubation (as judged by the intensity of the bands in the FTIR DS). Finally, the mixture incubated in D_2O was pelleted and used immediately.

Cells from *S. 6803* that could grow in 87% D_2O were prepared as described previously (Zybailov et al., 2000). PS I particles from the cells grown in D_2O were prepared using normal H_2O based buffers, as described (Zybailov et al., 2000). We show below that the use of H_2O buffers for sample preparation is unlikely to lead to any proton exchange. The extent of ^2H incorporation into PS I was assessed by comparing the intensity of the amide II absorbance band for ^1H and ^2H labeled PS I samples (see below). In the following we will refer to the PS I samples obtained from cells grown in H_2O/D_2O as $^1H/^2H$ labeled PS I samples. We will also refer to the corresponding spectra as $^1H/^2H$ FTIR DS.

Curve fitting was performed using the software package OPUS, supplied by Bruker Instruments (Billerica, MA), as described (Yang et al., 2002). The

FTIR DS were resolved into sums of combined Lorentzian and Gaussian component bands (plus a baseline) by means of a curve fitting algorithm that utilizes a Levenberg-Marquardt iteration procedure. The goodness of fit is quantified by an root mean-square (RMS) noise parameter. The smaller the RMS noise parameter the better the fit, or more accurately, the closer the fitted curve matches the data. This is important since it is not possible to visually inspect and judge how well the fitted curves match the data. For the $^1H/^2H$ data, the RMS error is $3.384 \times 10^{-4}/3.44 \times 10^{-4}$.

Simulations and figures for presentation from the PS I crystal structure (PDB file accession number IJB0) were performed using Swiss PdbViewer, v3.7b2 (http://www.expasy.ch/spdbv; Geux and Peitsch, 1997).

RESULTS

Fig. 3 shows typical IR absorption spectra obtained using PS I particles from *S. 6803*, under various sets of conditions. In Fig. 3 *A* the spectrum for ^1H labeled PS I samples is shown. It is also shown dotted in *B*–D. The band at 1654 cm^{-1} is due to amide I and water absorption. The shape of the 1654 cm^{-1} band therefore varies slightly with the water content of the sample. Fig. 3 *B* shows IR absorption spectra for PS I samples that have been incubated in H_2O and D_2O. These spectra have been considered in detail previously (Sivakumar et al., 2003), as have the corresponding light induced ($P700^+$-P700) FTIR DS. The inset in Fig. 3 shows the two spectra in *B* on an extended frequency scale, between 4000 and 1400 cm^{-1}. The bands in this region allow an estimation of the hydration state of the samples studied because the bands at ~2500/3300 cm^{-1} are due to D_2O/H_2O (amide A also contributes to the ~3300 cm^{-1} band). In measurements in our lab, we rarely use dehydrated samples. Thus we avoid any complications from spurious absorptions that could occur upon protein dehydration. In all measurements reported here, the absorption bands associated with D_2O/H_2O (~2500/3300 cm^{-1}) are well beyond 2.0 in absorbance units. The band near 3300 cm^{-1} in the inset is actually saturated, as it increases in intensity as the sample is dehydrated (data not shown). The actual absorbance of the 3300 cm^{-1} band shown in the inset is above 3.0 in absorbance units. In comparison to the hydrated sample conditions used here, the PS I samples used in the work reported by Kim et al. (2001) were almost completely dehydrated, as evidenced by the fact that the amide I absorption band in these samples was considerably more intense than either the D_2O or H_2O absorption bands at ~2500 or ~3300 cm^{-1}. The use of dehydrated samples could possibly explain why the ($P700^+$-P700) FTIR DS reported by Kim et al. do not closely resemble previously published ($P700^+$-P700) FTIR DS (Breton, 2001; Breton et al., 1999, 2002; Hastings et al., 2001).

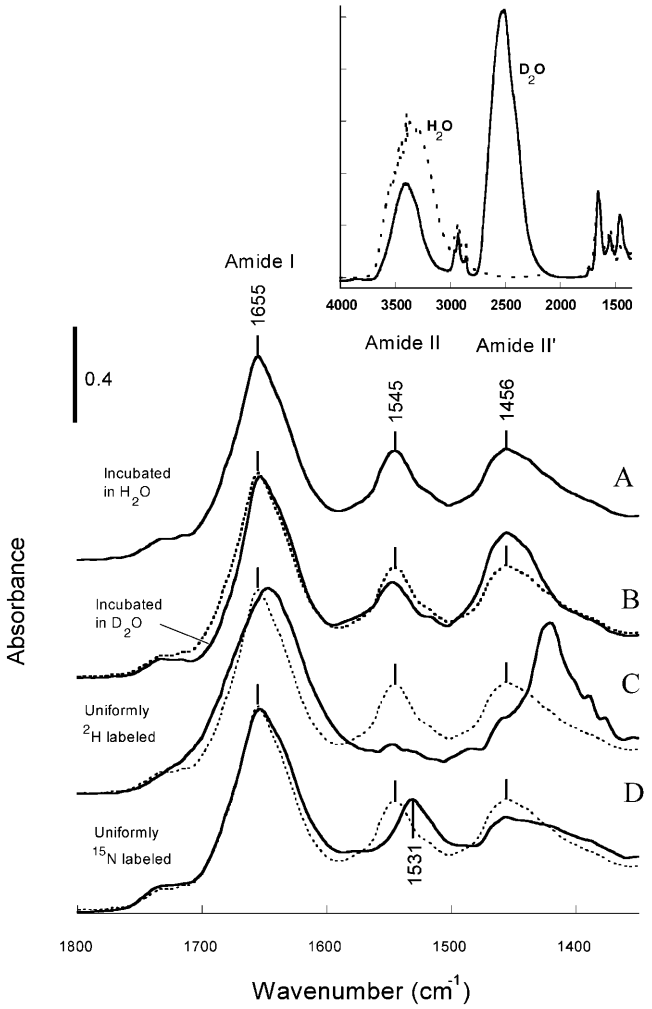

FIGURE 3 Infrared absorption spectra for the different PS I samples from *S. 6803*. (*A*) PS I samples incubated in H_2O buffer. This spectrum is also shown (*dotted*) in *B*–*D*. (*B*) PS I samples that have been extensively washed and incubated in D_2O buffer. (*C*) PS I samples, prepared in H_2O buffers but obtained from cells grown in D_2O. (*D*) PS I samples obtained from cells grown in ^{15}N labeled media. (*Inset*) Infrared absorption spectra in the 4000–1350 cm^{-1} region, for ^1H (*dotted*) and ^2H incubated (*solid*) PS I samples. These spectra are the same as the ones shown in *B*.

Fig. 3 *D* shows IR absorption spectra obtained using PS I particles that were obtained from cells grown in unlabeled media (^{14}N), and in media containing ^{15}N labeled nitrate. Upon ^{15}N labeling of the PS I particles the whole of the amide II absorption band downshifts from 1547 to 1532 cm^{-1}. Since the whole of the amide II absorption band shifts we conclude that ^{15}N has been incorporated into PS I at near the 100% level. The light induced ($P700^+$-P700) FTIR DS, in the 1770–1600 cm^{-1} spectral region, corresponding to the spectra in Fig. 3 *D*, are shown in Fig. 4. Direct subtraction of the ^{14}N FTIR DS from the ^{15}N FTIR DS results in the (^{14}N-^{15}N), isotope edited, FTIR double difference spectrum (DDS), which is also shown in Fig. 4. Clearly, uniform ^{15}N labeling of PS I does not greatly modify the ($P700^+$-P700) FTIR DS.

Fig. 3 *C* shows IR absorption spectra obtained using PS I particles that were obtained from cells grown in H_2O, and 87% D_2O. The corresponding light induced ($P700^+$-P700) FTIR DS, in the 1770–1600 cm^{-1} spectral region, are shown in Fig. 5. Direct subtraction of the ^2H spectrum from the ^1H spectrum results in the (^1H-^2H) isotope edited FTIR DDS,

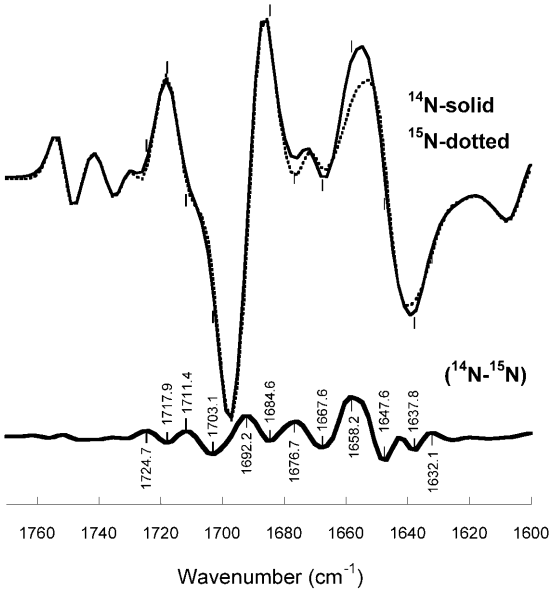

FIGURE 4 Light induced (P700$^+$-P700) FTIR DS in the 1770–1600 cm^{-1} spectral region, obtained using PS I particles that have been grown in ^{14}N (*solid*) and ^{15}N (*dotted*) labeled media. The (^{14}N-^{15}N) FTIR DDS is also shown.

which is also shown in Fig. 5. In Fig. 3 *C*, the amide II absorption band for ^{2}H labeled PS I samples is greatly diminished, compared to the spectrum for ^{1}H labeled samples. From a comparison of the area under the amide II absorption bands in Fig. 3 *C* we conclude that growth of *S. 6803* in 87% D_2O results in ~87% ^{2}H incorporation into PS I.

FTIR DS in the 1720–1670 cm^{-1} region are complex. To better resolve the component bands underlying the difference bands we have applied curve fitting procedures to the ^{1}H and

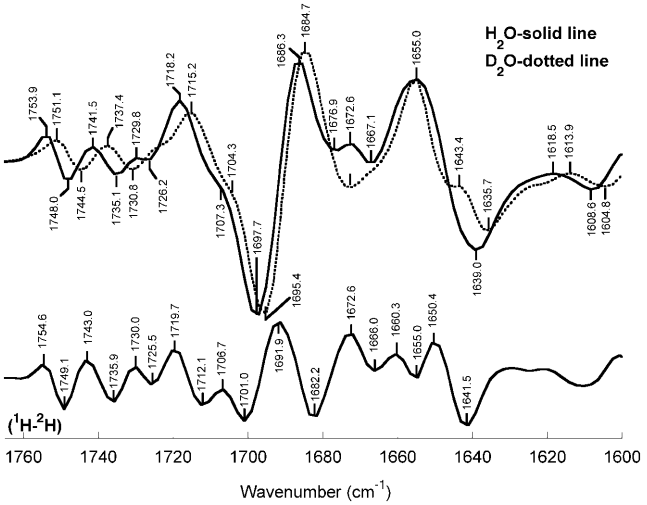

FIGURE 5 Light induced (P700$^+$-P700) FTIR DS in the 1770–1600 cm^{-1} spectral region, obtained using PS I particles that have been grown in H_2O (*solid*) and D_2O (*dotted*). The difference between the two spectra is also shown ((^{1}H-^{2}H) double difference spectrum).

^{2}H labeled FTIR DS in Fig. 5. The component bands derived from curve fitting, as well as the resultant fit to the spectra are shown in Fig. 6. The resulting curve fit parameters are summarized in Table 2.

Recently it has been suggested that SH modes associated with a cysteine residue contribute to (P700$^+$-P700) FTIR DS near 2560 cm^{-1} (Kim et al., 2001). To verify this result we collected (P700$^+$-P700) FTIR DS, using ^{1}H labeled PS I samples, in the 7000–1000 cm^{-1} spectral region. This FTIR DS is shown in Fig. 7. In addition to the broad absorption band centered near 3100 cm^{-1} we also observe a second broad band at ~5200 cm^{-1}. The origin of these broad difference bands is under investigation, and will not be discussed here. The inset in Fig. 7 shows an expanded view of the spectra in the 2580–2530 cm^{-1} spectral region. The noise level in the experiment is also shown in the inset. Clearly, we do not observe a difference band in this region that is significantly greater than the noise level. The length of

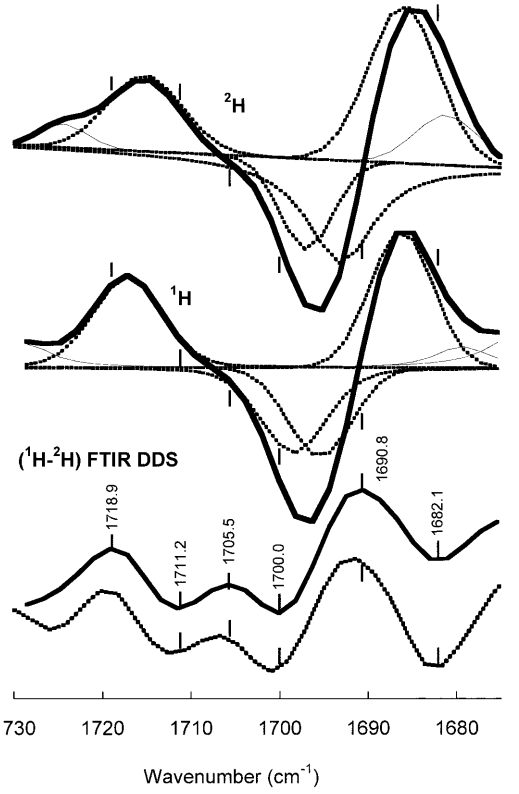

FIGURE 6 Results obtained from curve fitting the ^{2}H (*top*) and ^{1}H (*middle*) FTIR DS in the 1728–1674 cm^{-1} region. In the top and middle, the resultant fit is the thick line, and overlaps the experimental data. The four component bands of interest are shown as dotted lines in each spectrum. Other component bands on the periphery are shown as thin solid lines. The frequency and bandwidth of the four component bands discussed here are presented in bold text in Table 2. The experimental (^{1}H-^{2}H) FTIR DDS shown (*dotted*) is taken from Fig. 4. The (^{1}H-^{2}H) FTIR DDS derived from subtracting the sum of the four component difference bands for the ^{2}H labeled PS I spectrum from the sum of the four difference bands of the ^{1}H labeled PS I spectrum is shown also (*solid*).

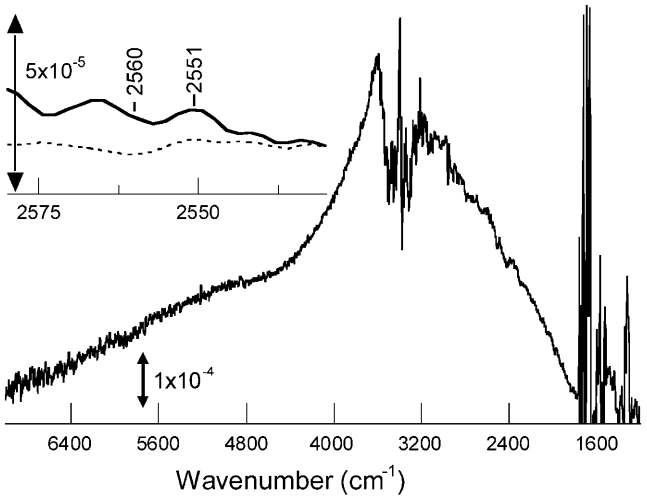

FIGURE 7 Light induced ($P700^+$-P700) FTIR DS in the 7000–1000 cm^{-1} spectral region, obtained using PS I particles that have been incubated in H_2O. (*Inset*) Expansion of the 2580–2530 cm^{-1} spectral region. The thin solid line is a dark-dark difference spectrum that gives a measure of the noise level in the experiment. The arrowed line in the inset gives an estimate of the peak/peak intensity of the difference band observed at 2560(−)/2551(+) cm^{-1} by Kim et al. (2001).

the solid double arrow in the inset in Fig. 7 represents the amplitude of the difference band observed near 2560 cm^{-1} by Kim et al. (2001). Between ~3100 and 3600 cm^{-1} the sample absorbance is considerably greater than 1.5 absorbance units (Fig. 3, *inset*). This explains the increased noise in the experimental data in this spectral region.

DISCUSSION

In all FTIR DS discussed in this article, no mediators were added to accept electrons from the iron sulfur clusters. Identical DS were observed when ferricyanide/ferrocyanide was used to accept electrons from the iron sulfur clusters (data not shown). This indicates that the FTIR DS shown here do not contain contributions from reduced iron sulfur clusters, and that all the bands are due to perturbations resulting because of $P700^+$ formation.

For the cells from *S. 6803* grown in 87% D_2O, PS I particles were prepared using H_2O buffers. It could therefore be possible that some ^2H to ^1H exchange has occurred for the samples that we call ^2H labeled. Two pieces of evidence argue against this, however. First, we have found that exchangeable protons do not modify the ($P700^+$-P700) FTIR DS (Sivakumar et al., 2003). Second, the amide II absorption bands in Fig. 3 *C* indicate close to 87% ^2H incorporation into PS I. From this observation we conclude that the use of ^1H_2O based buffers do not lead to decreased levels of ^2H incorporated into PS I.

The PS I particles from *S. 6803* used by Kim et al. (Kim and Barry, 2000; Kim et al., 2001) appear to be quite different from those studied by us, and others. First, the intense difference band at 1639(−)/1655 cm^{-1} in Fig. 5 (^1H spectrum) is diminished considerably in the spectra reported in Kim et al. (2001). The ratio of the peak/peak intensity of the 1698(−)/1718(+) and 1639(−)/1654 cm^{-1} difference bands in Fig. 5 is ~1.8. In contrast, Kim et al. (2001) observe an intensity ratio of ~3.8. Second, at room temperature, the shape and intensity of the broad positive band observed in the 5000–2000 cm^{-1} region (Fig. 7) is very different from that observed in Kim et al. (2001). At 80 K, the shape and intensity of the broad band observed by Kim et al. is also considerably different from that reported previously at 90 K (Breton et al., 1999). Third, Kim et al. observe a difference band at 2560(−)/2551(+) cm^{-1}, which they associate with an SH vibrational mode of a cysteine residue. This difference band is observed to increase in intensity as the temperature is lowered, and is affected by ^1H to ^2H exchange (Kim et al., 2001). We do not observe such a difference band at room temperature (Fig. 7, *inset*) or 77 K (G. Hastings, unpublished), and no such band was observed in spectra collected at 90 K (Breton et al., 1999). The origin of the above discrepancies are unresolved but it appears likely that the PS I particles from *S. 6803* used by us, and others (Breton, 2001; Breton et al., 1999, 2002), are different from those used by Kim et al. (2001), at least in terms of the ($P700^+$-P700) FTIR DS.

The 1770–1725 and 1725–1670 cm^{-1} spectral regions are referred to as the ester and keto C=O regions, respectively. Here we will consider both regions separately.

The ester C=O region

For isolated Chl-*a* in THF, the 13^3 and 17^3 ester C=Os absorb between 1735 and 1745 cm^{-1} (Katz et al., 1966, 1978; Nabedryk et al., 1990). From (Chl-a^+-Chl-*a*) electrochemically induced FTIR DS (Chl-*a* dissolved in THF), the 13^3 ester C=O was observed to absorb near 1742 cm^{-1} and upshift 12 cm^{-1} upon cation formation (Nabedryk et al., 1990). Although of very low intensity, a difference band at 1749(+)/1737(−) cm^{-1} was associated with the 17^3 ester C=O in these (Chl-a^+-Chl-*a*) FTIR DS (Nabedryk et al., 1990). Based on these studies it was suggested that the 1754(+)/1748(−) and 1742(+)/1735(−) cm^{-1} difference bands (Fig. 5) are due to a 6–7 cm^{-1} cation induced upshift of the 13^3 ester C=Os of P_B and P_A, respectively. Since the difference band assigned to the 13^3 ester C=O of P_A absorbs at lower frequency, it was suggested that it could be hydrogen bonded. The 2.5-Å crystal structure (Fromme et al., 2001; Jordan et al., 2001) indicates that it is the oxygen adjacent to the 13^3 ester C=O that could be H-bonded (Fig. 2). The fact that 13^3 ester C=O modes of both Chls of P700 are observable in the FTIR DS could indicate significant charge over both P_A and P_B in the $P700^+$ state. Although unlikely, we cannot entirely rule out the possibility that it is the charge on P_B that perturbs the 13^3 ester C=O of P_A. In addition, we cannot rule out the possibility that the 13^3 ester C=O of P_A becomes observable in the FTIR DS due to a cation induced

conformational change in the vicinity of the 13^3 ester C=O of P_A. For example, the ester oxygen could be H-bonded to the side chain of Thr-A743 in the ground state (Fig. 2). This H-bond is broken or otherwise modulated upon cation formation, perhaps because the hydroxyl group of Thr-A743 flips to form an H-bond with the 13^1 keto C=O of P_A (see below). Notice that this later mechanism does not depend on charge delocalization over P_A and P_B. For this later mechanism the charge could be predominantly localized on P_B. This mechanism therefore could agree with the results from ENDOR studies of PS I, which indicate that the majority of the charge (>85%) is located on P_B in the $P700^+$ state (Kass et al., 2001; Webber and Lubitz, 2001). This mechanism could also be in good agreement with the crystallographic data (Fig. 2; Fromme et al., 2001; Jordan et al., 2001).

The 13^3 ester C=O modes of P700 and $P700^+$ are unaltered upon incubation of PS I particles in D_2O (Sivakumar et al., 2003), indicating that H_2O-19 (Fig. 2) is not exchangeable. The 13^3 ester C=O modes of P700 and $P700^+$ are also little affected by uniform ^{15}N labeling of PS I (Fig. 4), indicating that the 13^3 ester C=O modes are uncoupled from the pyrrole nitrogens of P_A and P_B. The 13^3 ester C=O modes are significantly perturbed upon uniform ^2H labeling of PS I, however. The 1754(+)/1748(−) cm^{-1} difference band downshifts ~2.8(+)/3.5(−) cm^{-1} upon ^2H labeling, whereas the 1742(+)/1735(−) cm^{-1} difference band downshifts ~4.1(+)/4.3(−) cm^{-1} upon ^2H labeling. The weak difference band at 1730(+)/1726(−) cm^{-1} appears to downshift ~3.6(+)/4.0(−) cm^{-1} upon ^2H labeling (see Table 1). These band shifts are best discussed within the context of the (^1H-^2H) FTIR DDS in Fig. 5. When a complete difference band is shifted upon labeling, and the magnitude of the shift is less than the width of the difference band, then a second derivative type feature is expected in the isotope edited FTIR DDS. If the shift is greater than the width of the difference band then four features are expected in the FTIR DDS. The nature of the positive and negative features in the FTIR DDS depends on the direction of the difference band shifts. Thus the ^2H induced downshift of the 1754(+)/1748(−) cm^{-1} difference band (<4 cm^{-1}) gives rise to the 1755(+)/1749(−)/1743(+) cm^{-1} second derivative feature in the (^1H-^2H) FTIR DDS. Similarly, the 1742(+)/1735(−) cm^{-1} difference band downshifts (>4 cm^{-1}) upon uniform ^2H labeling. This downshifting difference band gives rise to the 1743(+)/1736(−)/1730(+) cm^{-1} second derivative feature in the (^1H-^2H) FTIR DDS. The 1743(+) cm^{-1} band in the (^1H-^2H) FTIR DDS is overlapped and due to features associated with both 13^3 ester C=Os of P700. This assignment of the 1743(+) cm^{-1} band in the (^1H-^2H) spectrum is appropriate since the 1743(+) cm^{-1} band is broader and slightly more intense than the 1755(+) cm^{-1} band in the (^1H-^2H) FTIR DDS.

The ^2H induced frequency shifts of the 13^3 ester C=O modes of P_A and P_B differ by 0.8–1.3 cm^{-1}, with the mode of P_B downshifting less than the corresponding mode of P_A. This difference is likely due to the fact that the oxygen adjacent to the 13^3 ester C=O of P_A is involved in H-bond network (Fig. 2), and that no corresponding H-bond pattern is observed for P_B.

Caution should be exercised when comparing ($P700^+$-P700) FTIR DS collected at RT and 90 K, since only ~40% of PS I particles are involved in reversible ET at 90 K (Schlodder et al., 1998). However, from (^1H-^2H) FTIR DDS collected at 90 K, the clearest observation is that a band at ~1754(+)/1749(−) cm^{-1} (probably due to the 13^3 ester C=O of P_B) downshifts ~5/7 cm^{-1} upon uniform ^2H labeling (Breton et al., 1999), which is significantly greater than our observations at RT.

The mechanism underlying the ^2H induced difference band downshifts of the 13^3 ester C=O modes of P_A and P_B is not entirely clear. One possibility is that the downshift is due to ^2H labeling of the 13^4 methyl hydrogens. However, in PS I from *S. 6803* at 264 K, the 1754(+)/1748(−) and 1742(+)/1735(−) cm^{-1} difference have been reported to downshifted by ~1/3 and ~2/2 cm^{-1} upon specific 13^4 methyl deuteration (Kim and Barry, 2000). Therefore, effects other than 13^4 methyl deuteration must also contribute to the downshifting 13^3 ester C=O modes of P_A and P_B.

In Fig. 5, a low intensity difference band at 1730(+)/1726(−) cm^{-1} is also downshifted by ~5 cm^{-1} upon ^2H labeling. The 1726(−) cm^{-1} feature in the (^1H-^2H) spectrum is likely associated with the ^2H induced shift of this difference band. The origin of the 1730(+)/1726(−) cm^{-1} difference band in the ^1H FTIR DS is unclear. It could be associated with another 13^3 ester C=O mode, or it could be associated with the 17^3 ester C=O mode. One point of note is that the 17^3 ester C=O difference band in (Chl-a^+-Chl-a) FTIR DS is extremely weak (Nabedryk et al., 1990). However, as discussed above, a cation induced conformational change in P_A could alter the 17^3 ester C=O, making it observable in ($P700^+$-P700) FTIR DS. Pertinent to this idea is that the 17^3 ester C=O is coupled to the H-bond network involving H_2O-19, via Ser-A607 and/or Tyr-A735 (Fromme et al., 2001; Jordan et al., 2001). If the 1730(+)/1726(−) cm^{-1} difference band is associated with the 17^3 ester C=O of

TABLE 1 Peak positions and assignments of difference bands associated with the 13^3 ester C=O modes in the ^1H and ^2H FTIR DS in Fig. 5

13^3 ester C=O modes of P700/$P700^+$			
D_2O	H_2O	^2H induced downshift	Assignment
1751.1(+)	1753.9(+)	2.8	P_B^+
1744.5(−)	1748.0(−)	3.5	P_B
1737.4(+)	1741.5(+)	4.1	P_A^+
1730.8(−)	1735.1(−)	4.3	P_A
1729.8(+)	~1724.5(+)	5.3	P_A^+
1726.2(−)	~1721.7(−)	4.5	P_A

P_A then the conclusion is that the H-bond network (Fig. 2) is modified upon cation formation. In addition, with the above assignments, there is no need to invoke any kind of ester C=O mode frequency heterogeneity to explain the difference and double difference spectra in Fig. 5. Previously, it was suggested that there are at least four distinguishable 13^3 ester C=O modes (Kim et al., 2001). However, our uniform ^2H labeling experiments provide no evidence to support this, and we conclude that there is no heterogeneity in the frequencies of the ester C=O modes of P700. The previous claim of four distinct 13^3 ester C=O modes from the two Chls of P700 probably arose from the fact that each derivative feature in the FTIR DDS was assigned to a distinct ester C=O mode. However, as we showed above, a shift of a complete difference band results in at least a second derivative feature (not a first derivative feature) in FTIR DDS.

The 13^1 keto C=O region

For ^1H labeled PS I particles from *S. 6803*, difference band features are observed at 1718(+), 1698(−), 1686(+), 1655(+), and 1639(−) cm^{-1}. A shoulder is also observed at ~1707 cm^{-1}, and weak features at 1677(−), 1673(+), and 1667(−) cm^{-1}. As outlined above, there are two opposing interpretations of the observed bands in ($P700^+$-P700) FTIR DS. 1), The 1698(−)/1718 and 1639(−)/1655(+) cm^{-1} difference bands are due to 13^1 keto C=O modes of P_B and P_A, respectively (Breton et al., 1999). It was also previously suggested that the whole of the 1698(−)/1718 cm^{-1} difference band is due to a pure C=O mode (Nabedryk et al., 1990; Tavitian et al., 1988). Within this interpretation of ($P700^+$-P700) FTIR DS, the 1686(+) cm^{-1} band was unassigned (Breton et al., 1999). 2), The 13^1 keto C=O modes of both P_B and P_A contribute to the 1698(−) cm^{-1} band (Hastings et al., 2001), and these modes of P_B/P_A upshift/downshift to 1718/1686 cm^{-1}, respectively, upon cation formation. The cation induced downshifting 13^1 keto C=O mode of P_A was attributed to a strengthening of the H-bond (decrease in H-bond length) from Thr-A743 (Fig. 2). The flipping of the H-bonding hydroxyl side chain of Thr-A743 between the ester oxygen and the 13^1 keto C=O, suggested above, is also consistent with a cation induced downshifting 13^1 keto C=O mode of P_A. In any case, the cation induced downshifting of 13^1 keto C=O mode of P_A is consistent with the idea that the H-bond network is modified upon cation formation. In addition to the above, we also suggested that the 1639(−)/1655(+) cm^{-1} difference band was assigned to modes associated with both of the histidines that provide axial ligands to P_A and P_B (His-B660 and His-A680). More specifically, the 1639(−)/1655(+) cm^{-1} difference band is due to (mixed) (Hasegawa et al., 2000) C=C modes of the imidazole side chain of the ligating histidines (Hastings et al., 2001).

Comparison of ester and keto C=O mode band shifts upon deuteration of PS I

Upon ^2H labeling the 1718(+)/1698(−)/1686(+) cm^{-1} difference bands downshift 3.0/2.3/1.7 cm^{-1}, respectively. The shoulder at 1707 cm^{-1} also downshifts ~3 cm^{-1} upon deuteration. On average, these shifts are less than the ^2H induced downshifts observed for the 13^3 ester C=O modes (Table 1). For deuterated Chl-*a* in THF, the 13^3 ester/13^1 keto C=O absorption bands were observed to downshift 5/3 cm^{-1} upon deuteration, respectively (Breton et al., 1999). That is, the ester C=O mode displays a greater ^2H induced downshift than the 13^1 keto C=O mode. Based on this observation for deuterated Chl-*a*, we assign the bands discussed in Table 2 to 13^1 keto C=O modes of the Chls of P700. If some of these features were associated with 13^3 ester C=O modes, the ^2H induced downshifts would be >3 cm^{-1}.

The smaller ^2H induced shifts of the keto C=O modes, compared to the ester C=O modes, also follows from the DDS in Fig. 5. From the ^1H FTIR DS, the 1718(+)/1698(−) cm^{-1} difference band is about a factor of 5 more intense than the 1754(+)/1748(−) cm^{-1} difference band. However, the intensity of the features in the DDS between 1720 and 1670 cm^{-1} are less than a factor of two larger than the features above 1720 cm^{-1}. This observation indicates that the bands in the 1720–1670 cm^{-1} region undergo reduced ^2H induced band shifts relative to the bands above 1720 cm^{-1}.

The 13^1 keto C=O modes of both P_A and P_B contribute to the 1698(−) cm^{-1} difference band

In the 1720–1670 cm^{-1} region the pattern of bands in the (^1H-^2H) FTIR DDS in Fig. 5 is somewhat similar to that reported previously for PS I particles from *S. 6803* at 90 K (Breton et al., 1999), although the (^1H-^2H) FTIR DS at 90 K were never interpreted. From ($P700^+$-P700) FTIR DS from *S. 6803* at 90 K, it is suggested that the 1698(−) cm^{-1}

TABLE 2 Curve fit parameters used to describe the ^1H and ^2H FTIR DS in Fig. 6

13^1 keto C=O modes of P700/$P700^+$ (from curve fitting)				
D_2O		H_2O		^2H induced downshift
Peak	Width	Peak	Width	
		1672.0	8.8	
1681.1	8.5	1679.4	7.3	
1686.0(+)	**9.2**	**1686.2(+)**	**8.2**	**0.2**
1693.1(−)	**9.2**	**1695.4(−)**	**8.4**	**2.3**
1697.0(−)	**7.0**	**1698.4(−)**	**8.9**	**1.4**
1715.2(+)	**9.9**	**1717.1(+)**	**9.1**	**1.9**
1724.5	6.6	1728.5	6.6	

The four bands shown dotted in Fig. 5 are the ones of interest. The parameters for these four bands are shown in bold text in the table. Further bands were included in the fit to simulate changes outside the region of interest, but are of little significance in this level of analysis. Fitting procedures used have been described (Yang et al., 2002).

difference band is due to the 13^1 keto C=O mode of P_B, which upshifts to 1716 cm^{-1} upon cation formation. However, since several features associated with 13^1 keto C=O modes appear between 1720 and 1670 cm^{-1} in the FTIR DDS in Fig. 5, this interpretation is incomplete and, as we suggested previously (Hastings et al., 2001), at least two species must contribute to the 1698(−) cm^{-1} difference band.

To better resolve the underlying component bands in the ^1H and ^2H FTIR DS, we have fit the spectra to a sum of component bands using a curve fitting procedure based on the Marquardt algorithm (the curve fitting procedures employed here have been described; Hastings et al., 2001; Yang et al., 2002). Fig. 6 shows the results of curve fitting the ^1H and ^2H FTIR DS in the 1728–1678 cm^{-1} region. In the curve fitting analysis the ~1698(−) cm^{-1} band consists of two underlying components; one downshifts the other upshifts upon $P700^+$ formation. We are primarily interested in these four component bands. However, further components on the periphery of the fitted frequency range have been included to simulate changes occurring outside this region of interest. The parameters derived from this curve fitting are outlined in Table 2. From Table 2 it appears that all bands in the keto C=O region (except the 1686 cm^{-1} band) downshift 1.4–2.3 cm^{-1} upon deuteration. In Fig. 6, the (^1H-^2H) FTIR DDS constructed using only the four component bands (two difference bands) in each of the ^1H and ^2H FTIR DS is shown (*dotted*, *bottom*). Notice that the 1711(−)/1706(+)/1700(−) cm^{-1} feature is reproduced in our constructed (^1H-^2H) FTIR DDS. Importantly, the 1711(−)/1706(+)/1700(−) cm^{-1} feature, along with the 1691(+)/1682(−) cm^{-1} feature, in the experimental (^1H-^2H) FTIR DDS, cannot be reproduced if the 1698 cm^{-1} difference band (^1H FTIR DS) is due to a single species. The model presented here is the simplest possible that can provide an explanation for the (^1H-^2H) FTIR DS in the 1730–1670 cm^{-1} region. So we conclude that in PS I from *S. 6803*, the 1698(−) cm^{-1} difference band is a composite of at least two underlying bands (at 1695 and 1698 cm^{-1} in the ^1H FTIR DS; see Table 2) that shift in opposite directions upon cation formation. Most likely the 1698 cm^{-1} component band upshifts to 1717 cm^{-1}, whereas the 1695 cm^{-1} component band downshifts to 1686 cm^{-1}, upon cation formation (Table 2).

In summary, a difference band near 1693(−) cm^{-1} downshifts 2.3 cm^{-1} upon deuteration (see Table 2). This gives rise to the 1695(+) cm^{-1} feature in the (^1H-^2H) FTIR DDS. This ^2H induced downshift probably also contributes partly to the 1701(−) cm^{-1} feature in the (^1H-^2H) FTIR DDS. In addition, a band at 1686(+) cm^{-1} downshifts slightly upon deuteration, giving rise to the 1682(−) cm^{-1} band in the FTIR DDS and partly contributing to the 1692(+) cm^{-1} band in the FTIR DDS. Finally, a positive difference band near 1717(+) cm^{-1} downshifts upon deuteration, giving rise to the 1719(+) and 1711(−) cm^{-1} features in the (^1H-^2H) FTIR DDS. The 1707(+)/1701(−) cm^{-1} feature in the (^1H-^2H) FTIR DDS is due in part at least to the differential shifting of the 1695(−) and 1698(−) cm^{-1} bands (by 2.3 and 1.4 cm^{-1}) upon deuteration. The magnitude of the ^2H induced frequency downshift of the two bands that underlie the 1698 cm^{-1} band (2.3/1.4 cm^{-1}; see Table 2) are consistent with both bands being associated with 13^1 keto C=O modes. The fact that the 1698/1695 cm^{-1} bands (^1H FTIR DS) shift in opposite directions upon cation formation could be related to the fact that the H-bond network is modified upon cation formation, as discussed above. That is, it is possible that the 13^1 keto C=O of P_A is not H-bonded in the ground state, but it is upon cation formation.

The ^2H induced downshift of the two bands that underlie the 1698 cm^{-1} band could be consistent with the idea that one of the component bands is associated with a protein mode. For PS I, the amide I absorption band shifts ~2 cm^{-1} upon ^2H incorporation (Rath et al., 1998). However, the changes in amide I generally give rise to features well below 1698 cm^{-1}. In addition, protein modes generally give rise to features in FTIR DS that are significantly less intense than bands associated with C=O modes of the Chls. Given the large intensity of the component bands, underlying the 1698 cm^{-1} band, it is therefore unlikely that part of the 1698(−) cm^{-1} band is associated with a protein mode. In addition, if part of the 1698 cm^{-1} band (^1H spectrum) were due to a protein mode, then larger changes would be expected in the (^{14}N-^{15}N) DDS in Fig. 4, as amide I bands display a ^{15}N induced downshift of ~3 cm^{-1} (Breton et al., 1999), due to coupling of the C=O and CN modes (amide I absorption in proteins consists of contributions from the peptide C=O (~80%) and C-N groups (~20%)). Given the intensity of the bands in the (^{14}N-^{15}N) DDS, we have estimated that the component bands, underlying the 1698 cm^{-1} band, must shift less than 0.2 cm^{-1} upon ^{15}N labeling.

It is also unlikely that one of the component bands underlying the 1698 cm^{-1} band is due to an amino acid side-chain mode. Protonated carboxylic acid C=O modes usually absorb well above 1700 cm^{-1}. Even if a protonated carboxylic acid C=O mode did absorb near 1700 cm^{-1}, there are no such amino acids near P700 (Fromme et al., 2001; Jordan et al., 2001). In addition, ^2H labeling results in a 10–15 cm^{-1} downshift of carboxylic acid C=O modes (Siebert et al., 1982). Side-chain C=O modes of glutamine and asparagine could occur near 1700 cm^{-1} (Barth, 2000); however, again there is no evidence from the crystal structure to support this. Therefore, the weight of experimental evidence strongly supports the idea that the two component bands underlying the 1698 cm^{-1} band in ($P700^+$-P700) FTIR DS are due to 13^1 keto C=Os of both P_A and P_B.

Can the 13^1 keto C=O mode of P_A contribute to the 1639(−)/1655(+) difference band?

Given the above assignment, the question as to the origin of the 1639(−)/1655(+) cm^{-1} difference band arises. If the 1639(−)/1655(+) cm^{-1} difference band is due to the 13^1

keto C=O of P_A that it is strongly H-bonded (Breton et al., 1999), then this band is expected to downshift upon ^2H labeling. The precise downshift will depend on the strength of the H-bond and the extent of coupling between the OH and C=O modes. OH and C=O modes have very different frequencies, so the coupling is expected to be small. Upon deuteration the OH mode is considerably lowered in frequency, so significant changes in (the admittedly small) coupling are expected upon deuteration. From 1-D normal mode calculations (considering only force constants and masses; see Fig. 8 *B*) and density functional calculations of simple model molecules, we have found that a 2–3 cm^{-1} shift of the 13^1 keto C=O mode upon deuteration of the Thr-A743 hydroxyl group appears reasonable, especially given the fact that the H-bond must be very strong (G. Hastings, unpublished data). The situation encountered here (how C=O mode frequencies shift upon deuteration of coupled hydroxyl groups) (Fig. 8 *B*) is somewhat similar to how deuteration effects manifest themselves in carboxylic acids (Fig. 8 *A*). In protonated carboxylic acids it is well known that the C=O mode downshifts 10–15 cm^{-1} upon deuteration of the hydroxyl proton (Fig. 8 *A*) (Maeda et al., 1992; Nabedryk et al., 1995; Rothschild, 1992). Finally, it could also be possible that several of the O–O bond distances in Fig. 2 could change by 1–2% upon deuteration (Jeffrey, 1997). It is not at all clear if this could impact the 13^1 keto C=O mode, leading to resolvable frequency up- or downshifts. In the following we will make the (usual) assumption that deuterium induced changes in bond lengths are negligible.

An ~2–3 cm^{-1} downshift of the complete 1639(−)/1655(+) cm^{-1} difference band would result in a clear second derivative feature in the (^1H-^2H) FTIR DDS. Upon ^2H labeling the 1639(−)/1655(+) cm^{-1} difference band in the ^1H FTIR DS is modified, but a single intense difference band is still observed at 1636(−)/1655(+) cm^{-1} in the ^2H spectrum (Fig. 5). These changes give rise to a single derivative feature at 1650(+)/1642(−) cm^{-1} in the (^1H-^2H) FTIR DDS. The lack of any clear second derivative features in the (^1H-^2H) DDS indicates that the species responsible for the 1639(−)/1655(+) cm^{-1} difference band in the ^1H spectrum does not downshift ~2–3 cm^{-1} upon ^2H labeling of PS I. These observations therefore indicate that the 1639(−)/1655(+) cm^{-1} difference band is likely not due to a strongly H-bonded 13^1 keto C=O mode of P_A. The single derivative feature at 1650(+)/1642(−) cm^{-1} in the (^1H-^2H) DDS suggests the gain or loss of a single difference band upon ^2H labeling. It could also be due to ^2H induced intensity change of a whole difference band. The shape of the bands in the ^1H and ^2H FTIR DS and the (^1H-^2H) DDS suggest the former rather than the latter. The gain or loss of a difference band upon labeling (rather than a difference band shift) suggests that the 1650(+)/1642(−) cm^{-1} feature in the (^1H-^2H) DDS is due to one or more protein modes. The frequency of the feature is exactly in the region where one expects to observe difference bands associated with amide I modes.

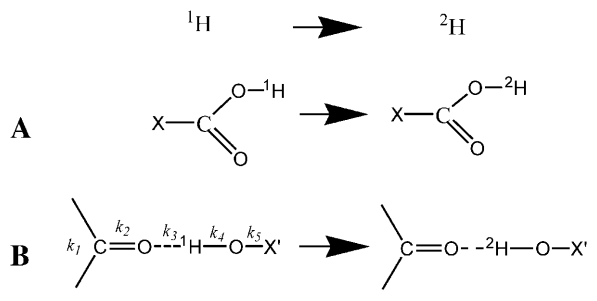

FIGURE 8 Comparison of deuteration effects expected on C=O modes of (*A*) a carboxylic acid and (*B*) a C=O mode H-bonded to a hydroxyl group. $k_{1...n}$ represent the force constants between the various atoms.

Do histidine modes contribute to the 1639(−)/1655(+) difference band?

If the 1650(+)/1642(−) cm^{-1} derivative feature in the (^1H-^2H) DDS is due to protein modes then the origin of the 1636(−)/1655(+) cm^{-1} difference band in the ^2H FTIR DS still needs to be addressed. Previously, we suggested that the 1639(−)/1655(+) cm^{-1} difference band (in *C. reinhardtii*) could be due to the C_4=C_5 stretching modes of the imidazole side chain of both of the histidine ligands (see Fig. 9 for imidazole numbering) (Hastings et al., 2001). This suggestion was partly based on the results from FTIR experiments and density functional calculations on various protonated forms of 4-methyl imidazoles, where it was shown that doubly protonated imidazole (imidazolium) displays a very intense absorption band at 1633 cm^{-1} (Hasegawa et al., 2000). Clearly the imidazole ring of the P700 ligating histidines is not doubly protonated (Fig. 9). However, the suggestion was that imidazolium could be electronically similar to imidazole that is ligated at N_1 and protonated at N_3 (Fig. 9). Support for this idea has come from quantum chemical calculations of zinc-bound 4-methyl imidazoles, where it has been shown that the C_4=C_5 mode increases considerably in frequency upon metal binding (Hasegawa et al., 2002).

In the quantum chemical calculations of 4-methyl imidazoles, it is found that the C_4=C_5 mode is mixed with NH modes of the imidazole side chain (Hasegawa et al., 2000, 2002). Since there is a coupling of imidazole C=C and NH modes, one might expect small changes in the 1639(−)/1655(+) cm^{-1} difference band upon ^{15}N labeling. The magnitude of the features in the (^{14}N-^{15}N) DDS in Fig. 4 do indicate small ^{15}N induced alterations in the 1639(−)/1655(+) cm^{-1} difference band. These changes may be consistent with the 1639(−)/1655(+) cm^{-1} difference band being due to coupled C_4=C_5/NH stretching modes of the imidazole side chain of both of the histidine ligands. However, it is not clear how to assign the bands in the (^{14}N-^{15}N) FTIR DDS.

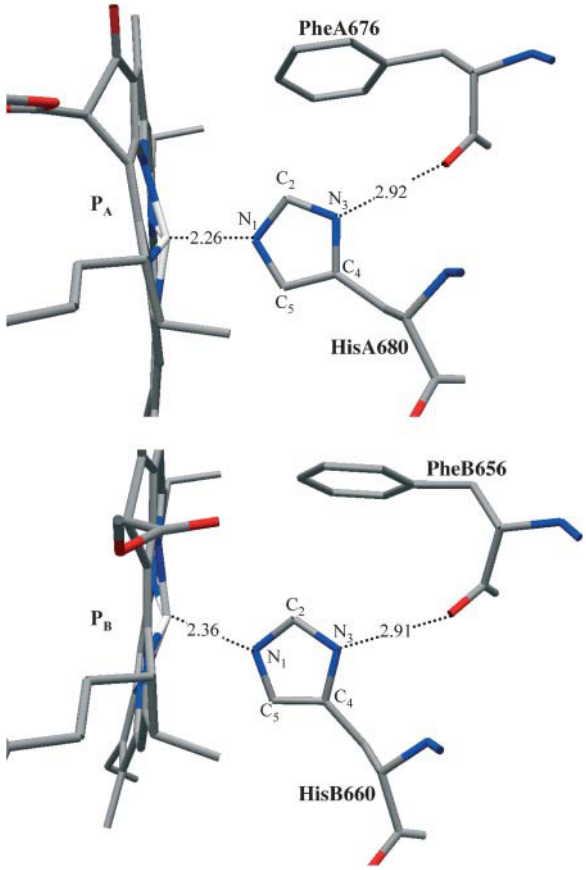

FIGURE 9 (*Top/bottom*) View of P_A/P_B showing the imidazole side chains of His-A680/His-B660 and possible interactions of the imidazole nitrogens. Figures were generated using Swiss PDBViewer and the crystallographic coordinates of PS I at 2.5-Å resolution (PDB file accession number IJB0).

For coupled $C_4{=}C_5$/NH imidazole modes one could also expect considerable ^2H induced band shifts: from quantum chemical calculations of zinc-bound 4-methyl imidazole protonated at N_3, it has been shown that deuteration of the N_3 proton leads to a considerable downshift in frequency (17 cm^{-1}) of the $C_4{=}C_5$ mode (Hasegawa et al., 2002). Fig. 9 shows that the N_3 proton of the side-chain imidazoles of both ligating histidines could be involved in H-bonding. So the situation is slightly different from the molecular system studied by (Hasegawa et al., 2002). Nevertheless, a downshift in frequency of the $C_4{=}C_5$ modes would still be expected upon deuteration. On the basis of the ^2H labeling experiments (Fig. 5), and consideration of calculations performed using zinc-bound methyl imidazoles as a test system (Hasegawa et al., 2002), it would appear that the 1639(−)/1655(+) cm^{-1} difference band cannot be due to imidazole modes of the histidine ligands. Thus, neither hypothesis as to the origin of the 1639(−)/1655(+) cm^{-1} difference band can be easily interpreted on the basis of the results presented here. One of the problems may be that multiple protein modes contribute to the spectra in the 1670–1630 cm^{-1} region. In the model presented above we suggest significant alteration in the H-bond network, which could result in multiple conformational changes of the protein backbone upon cation formation. The H-bond network involves multiple hydrogen atoms, all of which can be deuterated. This could lead to many changes in the spectra upon ^2H labeling, making interpretation very difficult. However, as discussed above, it is unlikely that the 1639(−)/1655(+) cm^{-1} difference band is associated with a strongly H-bonded C=O mode of P_A, since this mode can be readily accommodated and interpreted as being associated with part of the 1698 cm^{-1} difference band.

Very recently, Breton et al. (2002) have studied a series of site directed mutants from *S. 6803* in which the axial histidine to P_B has been changed to cysteine, glutamine, or leucine. In these mutants the 1639(−)/1655(+) cm^{-1} band of wild-type (WT) appears to be considerably modified. For the least disruptive glutamine mutation the 1639(−)/1655(+) cm^{-1} band of WT is decreased in intensity by ~10%, and considerably altered in shape. For the leucine mutant the 1639(−)/1655(+) cm^{-1} band of WT appears to increase considerably in intensity (by ~20%). These observations suggest significant modification of the protein backbone upon mutation of the B-side axial histidine. Without (WT-mutant) FTIR DDS it is impossible to unambiguously distinguish between changes in the spectra that result from the loss of histidine modes in the mutant, or from modification of the protein environment due to the mutation. Breton et al. (2002) also studied PS I particles from *S. 6803* in which only the histidines in the complex had been labeled with ^{13}C. However, no spectra in the 1660–1630 cm^{-1} region were presented for these particles.

Further considerations concerning the origin of the 1639(−)/1655(+) difference band?

If the 1639(−)/1655(+) cm^{-1} difference band of WT (in *S. 6803*) is due to the 13^1 keto C=O of P_A that is strongly H-bonded to Thr-A743, then removal of this H-bond should cause a dramatic upshift of this difference band. We have used FTIR DS to analyze a mutant from *C. reinhardtii* in which Thr-A739 (Thr-A743 in *S. elongatus*) is changed to alanine, and we find that the spectra cannot be consistently interpreted if the 1639(−)/1655(+) cm^{-1} difference band of WT is due to the 13^1 keto C=O of P_A (Wang et al., 2003). In contrast, Witt et al. (2002) also produced FTIR DS for mutants from *C. reinhardtii* in which Thr-A739 was mutated to Y, H, or V. These authors, however, did come to the conclusion that the 1639(−)/1655(+) cm^{-1} difference band of WT is due to the 13^1 keto C=O of P_A. It is difficult to analyze the origin of bands in the spectra of Witt et al. because no (WT-mutant) FTIR DDS were considered. In addition, as pointed out by Breton et al. (2002), these authors did not consider how mutation induced changes in the protein would impact their FTIR DS, and therefore their conclusion is premature. As mentioned above, we have analyzed

($P700^+$-P700) FTIR DS, obtained using a mutant from *C. reinhardtii* in which Thr-A739 is changed to alanine, in great detail, and we find that the spectra cannot be consistently interpreted if the 1639(−)/1655(+) cm^{-1} difference band of WT is due to the 13^1 keto C=O of P_A.

CONCLUSIONS

Several conclusions can be drawn from the data presented here: 1), The 13^3 ester and 13^1 keto C=O modes of P_A and P_B are not heterogeneously distributed in frequency. 2), Cysteine modes do not contribute to ($P700^+$-P700) FTIR DS. 3), More than one species contributes to the ~1698(−) cm^{-1} difference band in ^1H FTIR DS for WT PS I. The most likely conclusion is that it is the 13^1 keto C=O modes of P_A and P_B both contribute to the ~1698(−) cm^{-1} difference band. 4), The 13^1 keto C=O mode of P_A does not contribute to the 1639(−) cm^{-1} difference band in WT ^1H FTIR DS. 5), It is not clear if histidine modes contribute to the 1639 cm^{-1} difference band in WT ^1H FTIR DS.

This work was supported by start-up funds, a quality improvement grant, and a research initiation grant to G.H. from Georgia State University. G.H. also acknowledges support from the United States Department of Agriculture (grant 35318-10894).

REFERENCES

Barth, A. 2000. The infrared absorption of amino acid side chains. *Prog. Biophys. Mol. Biol.* 74:141–173.

Breton, J. 2001. Fourier transform infrared spectroscopy of primary electron donors in type I photosynthetic reaction centers. *Biochim. Biophys. Acta.* 1507:180–193.

Breton, J., E. Nabedryk, and W. Leibl. 1999. FTIR study of the primary electron donor of photosystem I (P700) revealing delocalization of the charge in P700(+) and localization of the triplet character in (3)P700. *Biochemistry.* 38:11585–11592.

Breton, J., W. Xu, B. A. Diner, and P. R. Chitnis. 2002. The two histidine axial ligands of the primary electron donor chlorophylls (P700) in photosystem I are similarly perturbed upon P700+ formation. *Biochemistry.* 41:11200–11210.

Brettel, K. 1997. Electron transfer and arrangement of the redox cofactors in photosystem I. *Biochim. Biophys. Acta.* 1318:322–373.

Fromme, P., P. Jordan, and N. Krauss. 2001. Structure of photosystem I. *Biochim. Biophys. Acta.* 1507:5–31.

Geux, N., and M. C. Peitsch. 1997. SWISSMODEL and SWISSPDB VIEWER: an environment for protein modelling. *Electrophoresis.* 18:2714–2723.

Golbeck, J. H., and D. Bryant. 1991. Photosystem I. *In* Current Topics in Bioenergetics. C. P. Lee, editor. Academic Press, New York. 83–177.

Guergova-Kuras, M., B. Boudreaux, A. Joliot, P. Joliot, and K. Redding. 2001. Evidence for two active branches for electron transfer in photosystem I. *Proc. Natl. Acad. Sci. USA.* 98:4437–4442.

Hasegawa, K., T. Ono, and T. Noguchi. 2000. Vibrational spectra and ab initio DFT calculations of 4-methylimidazole and its different protonation forms: Infrared and Raman markers of the protonation state of a histidine side chain. *J. Phys. Chem. B.* 104:4253–4265.

Hasegawa, K., T. Ono, and T. Noguchi. 2002. Ab initio density functional theory calculations and vibrational analysis of zinc-bound 4-methylimidazole as a model of a histidine ligand in metalloenzymes. *J. Phys. Chem. A.* 106:3377–3390.

Hastings, G., S. Hoshina, A. Webber, and R. Blankenship. 1995a. Universality of energy and electron transfer processes in photosystem I. *Biochemistry.* 34:15512–15522.

Hastings, G., L. Reed, S. Lin, and R. Blankenship. 1995b. Excited state dynamics in photosystem I: effects of detergent and excitation wavelength. *Biophys. J.* 69:2044–2055.

Hastings, G., V. M. Ramesh, R. Wang, V. Sivakumar, and A. Webber. 2001. Primary donor photo-oxidation in photosystem I: a re-evaluation of (P700(+) - P700) Fourier transform infrared difference spectra. *Biochemistry.* 40:12943–12949.

Jeffrey, G. 1997. An Introduction to Hydrogen Bonding. D. Truhlar, editor. Oxford University Press, New York, Oxford.

Joliot, P., and A. Joliot. 1999. In vivo analysis of the electron transfer within photosystem I: are the two phylloquinones involved? *Biochemistry.* 38:11130–11136.

Jordan, P., P. Fromme, H. T. Witt, O. Klukas, W. Saenger, and N. Krauss. 2001. Three-dimensional structure of cyanobacterial photosystem I at 2.5 angstrom resolution. *Nature.* 411:909–917.

Kass, H., P. Fromme, H. T. Witt, and W. Lubitz. 2001. Orientation and electronic structure of the primary donor radical cation P-700(+center dot) in photosystem I: a single crystals EPR and ENDOR study. *J. Phys. Chem. B.* 105:1225–1239.

Kass, H., W. Lubitz, G. Hartwig, H. Scheer, D. Noy, and A. Scherz. 1998. ENDOR studies of substituted chlorophyll cation radicals. *Spectrochim. Acta. A.* 54:1141–1156.

Katz, J. J., R. C. Dougherty, and L. Boucher. 1966. Infrared and nuclear magnetic resonance spectroscopy of chlorophyll. *In* The Chlorophylls. L. P. Vernon and G. R. Seely, editors. Academic Press, New York. 185–251.

Katz, J. J., L. Shipman, T. Cotton, and T. R. Janson. 1978. Chlorophyll agregation: coordination interactions in chlorophyll monomers, dimers and oligomers. *In* The Porphyrins. Physical Chemistry, Part C. D. Dolphin, editor. Academic Press, New York. 402–458.

Kim, S., and B. A. Barry. 2000. Identification of carbonyl modes of P700 and $P700^+$ by in situ chlorophyll labeling in photosystem I. *J. Am. Chem. Soc.* 122:4980–4981.

Kim, S., C. A. Sacksteder, K. A. Bixby, and B. A. Barry. 2001. A reaction-induced FT-IR study of cyanobacterial photosystem I. *Biochemistry.* 40:15384–15395.

Krabben, L., E. Schlodder, R. Jordan, D. Carbonera, G. Giacometti, H. Lee, A. N. Webber, and W. Lubitz. 2000. Influence of the axial ligands on the spectral properties of P700 of photosystem I: a study of site-directed mutants. *Biochemistry.* 39:13012–13025.

Maeda, A., J. Sasaki, Y. Shichida, T. Yoshizawa, M. Chang, B. Ni, R. Needleman, and J. K. Lanyi. 1992. Structures of aspartic acid-96 in the L and N intermediates of bacteriorhodopsin: analysis by Fourier transform infrared spectroscopy. *Biochemistry.* 31:4684–4690.

Nabedryk, E., J. Breton, R. Hienerwadel, C. Fogel, W. Mantele, M. L. Paddock, and M. Y. Okamura. 1995. Fourier transforms infrared difference spectroscopy of secondary quinone acceptor photoreduction in proton transfer mutants of *Rhodobacter sphaeroides*. *Biochemistry.* 34:14722–14732.

Nabedryk, E., M. Leonhard, W. Mantele, and J. Breton. 1990. Fourier transform infrared difference spectroscopy shows no evidence for an enolization of chlorophyll a upon cation formation either in vitro or during P700 photooxidation. *Biochemistry.* 29:3242–3247.

Rath, P., W. J. DeGrip, and K. J. Rothschild. 1998. Photoactivation of rhodopsin causes an increased hydrogen-deuterium exchange of buried peptide groups. *Biophys. J.* 74:192–198.

Redding, K., F. MacMillan, W. Leibl, K. Brettel, J. Hanley, A. W. Rutherford, J. Breton, and J. D. Rochaix. 1998. A systematic survey of conserved histidines in the core subunits of Photosystem I by site-directed mutagenesis reveals the likely axial ligands of P700. *EMBO J.* 17:50–60.

Rothschild, K. J. 1992. FTIR difference spectroscopy of bacteriorhodopsin: toward a molecular model. *J. Bioenerg. Biomembr.* 24:147–167.

Schlodder, E., K. Falkenberg, M. Gergeleit, and K. Brettel. 1998. Temperature dependence of forward and reverse electron transfer from A1-, the reduced secondary electron acceptor in photosystem I. *Biochemistry*. 37:9466–9476.

Siebert, F., W. Mantele, and W. Kreutz. 1982. Evidence for the protonation of two internal carboxylic groups during the photocycle of bacteriorhodopsin. *FEBS Lett*. 141:82–87.

Sivakumar, V., R. Wang, and G. Hastings. 2003. Photo-oxidation of P740, the primary electron donor in photosystem I from *Acaryochloris marina*. *Biophys. J*. 85:3162–3172.

Tavitian, B. A., E. Nabedryk, A. Wollenweber, W. Mantele, and J. Breton. 1988. FTIR spectroscopy of primary photosynthetic reactions in the two photosystems of green plants. Comparison with spectroelectrochemistry of chlorophyll models. *In* Spectroscopy Of Biological Molecules—New Advances. E. Schmid, F. Schneider, and F. Siebert, editors. Wiley and Sons, Chichester, UK. 297–300.

Wang, R., V. Sivakumar, Y. Li, K. Redding, and G. Hastings. 2003. Mutation induced modulation of hydrogen bonding to P700 studied using FTIR difference spectroscopy. *Biochemistry*. 42:9889–9897.

Webber, A. N., and W. Lubitz. 2001. P700: the primary electron donor of photosystem I. *Biochim. Biophys. Acta*. 1507:61–79.

Witt, H., E. Scholdder, C. Teutloff, J. Niklas, E. Bordignon, D. Carbonera, S. Kohler, A. Labahn, and W. Lubitz. 2002. Hydrogen bonding to P700: site-directed mutagenesis of threonine A739 of photosystem I in Chlamydomonas reinhardtii. *Biochemistry*. 41:8557–8569.

Yang, J. J., H. Yang, Y. Ye, H. Hopkins, Jr., and G. Hastings. 2002. Temperature-induced formation of a non-native intermediate state of the all beta-sheet protein CD2. *Cell Biochem. Biophys*. 36:1–18.

Zybailov, B., A. van der Est, S. G. Zech, C. Teutloff, T. W. Johnson, G. Shen, R. Bittl, D. Stehlik, P. R. Chitnis, and J. H. Golbeck. 2000. Recruitment of a foreign quinone into the A(1) site of photosystem I. II. Structural and functional characterization of phylloquinone biosynthetic pathway mutants by electron paramagnetic resonance and electron-nuclear double resonance spectroscopy. *J. Biol. Chem*. 275: 8531–8539.